Anisotropy-driven spin glass transition in the kagome antiferromagnet hydronium jarosite, $(H_3O)Fe_3(SO_4)_2(OH)_6$

2008 J. Phys.: Condens. Matter 20 452204

(http://iopscience.iop.org/0953-8984/20/45/452204)

IOP FTC
IOP PUBLISHING JOURNAL OF PHYSICS: CONDENSED MATTER
J. Phys.: Condens. Matter **20** (2008) 452204 (5pp) doi:10.1088/0953-8984/20/45/452204

FAST TRACK COMMUNICATION

Anisotropy-driven spin glass transition in the kagome antiferromagnet hydronium jarosite, $(H_3O)Fe_3(SO_4)_2(OH)_6$

W G Bisson[1] **and A S Wills**[1,2]

[1] Department of Chemistry, University College London, 20 Gordon Street, London WC1H 0AJ, UK
[2] The London Centre for Nanotechnology, 17-19 Gordon Street, London WC1H 0AH, UK

Received 2 September 2008, in final form 20 September 2008
Published 17 October 2008
Online at stacks.iop.org/JPhysCM/20/452204

Abstract
Highly frustrated systems have degenerate ground states that lead to novel properties. In magnetism the consequences of frustration underpin exotic and technologically important effects, such as high temperature superconductivity, colossal magnetoresistance, and the anomalous Hall effect. One of the enduring mysteries of highly frustrated magnetism is why certain experimental systems have a spin glass transition that is not determined by the strength of the dominant magnetic interactions. In this article we show that the spin glass transition in the kagome antiferromagnet hydronium jarosite arises from a coherent anisotropic distortion driven by solvation effects during synthesis. This finding could simplify treatment of the complex spin glass dynamics and has implications far beyond magnetism, as spin glasses provide important models for the out-of-equilibrium dynamics in other frustrated systems.

(Some figures in this article are in colour only in the electronic version)

Engineering highly degenerate electronic ground states provides a means to explore much of the exotic physics that has captivated modern science, particularly in the condensed matter [1–3]. The simplest examples of frustration come from magnetism where it can be a simple consequence of the geometry of the system. Such 'geometrically frustrated' magnets have been found to display a rich array of ground states and, more subtly, ordering mechanisms. Model systems include in the rare earth magnets, such as gadolinium gallium garnet (GGG) [4–6] and the pyrochlores, e.g. $Gd_2T_2O_7$ [7–10], $Gd_2Sn_2O_7$ [8, 11], $Er_2Ti_2O_7$ [12, 13], $Y_2Mo_2O_7$ [14–16]. Good model magnets based on transition metal ions are less common as their more extended electronic orbitals make them susceptible to structural distortions that relieve the frustration. Limiting the discussion to those that do not show such distortions, examples include the AB_2X_4 cubic spinels [17–26]; $SrCr_{9x}Ca_{12-9x}O_{19}$ [27, 28] and the related $Ba_2Sn_2Ga_3ZnCr_7O_{22}$ [29]; the puckered kagome 'staircases' $Ni_3V_2O_8$ and $Co_3V_2O_8$ [30–32]; the jarosites [33–36]; and the paratacamite-based materials [37–40]. Recently, artificial magnetic arrays, such as the dipolar spin ices [41–44], have been made that allow new possibilities for engineered Hamiltonians to be developed.

A long-standing question surrounds the observation of spin glass-like states in highly frustrated systems, and whether they result from disordered magnetic sites or bonds [14–16, 45], as they are in conventional spin glasses [46]. In this article we explore the crystallography of the model kagome antiferromagnet (KAFM) hydronium jarosite and show that it is anisotropy, and not random disorder, that stabilizes the glassy magnetic phase. Our findings support a model where the zero modes of the KAFM are pushed to finite energy by anisotropy, leading to a glassy magnetic phase [47].

Geometric frustration is exemplified by three antiferromagnetically coupled spins that form a triangle, as the geometry prevents a ground state in which all neighbouring moments are related by 180°. Instead a compromise configuration occurs where the spins are mutually oriented at 120°. There are two degenerate ground states that are distinguished by their

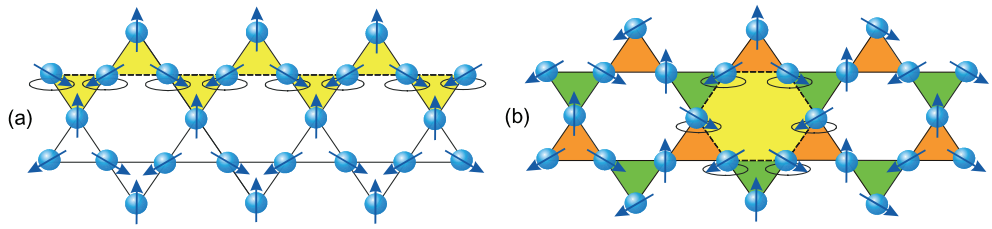

Figure 1. The different chiralities and spin folds possible for the kagome antiferromagnet. In (a) all the triangles have the $\kappa = +1$, while (b) shows a configuration with staggered $\kappa = -1$ chiralities. Zero-energy excitations termed 'spin folds' (highlighted in yellow) can occur within structures with both uniform and staggered chiralities: (a) shows a 'closed spin fold' based upon a magnetic lattice with staggered chirality (the $\sqrt{3} \times \sqrt{3}$ structure); (b) shows an 'open spin fold', which traverses a lattice if based upon the uniform chirality (the $q = 0$ structure).

chirality, defined by the clockwise vector products of spins, κ:

$$\kappa = \frac{2}{3\sqrt{3}}[\mathbf{S}_1 \times \mathbf{S}_2 + \mathbf{S}_2 \times \mathbf{S}_3 + \mathbf{S}_3 + \mathbf{S}_1]. \qquad (1)$$

This degeneracy is enhanced by vertex sharing the triangles to form the two-dimensional (2D) kagome network (figure 1), as the low connectivity of the lattice prevents the rule of a 120° ground state configuration from defining a coherent ground state. A degenerate manifold is formed that is 'connected', i.e. any ground state can be converted into any other through a series of collective zero-energy spin reorientations. Termed 'spin folds' [47], these are lines of two sublattices that rotate about the axis defined by the third sublattice. Planar anisotropy creates an energy cost to spin reorientations out of the kagome plane, and retards the fluid motion of spin folds, giving rise to the spin glass state. The spin glass transition then corresponds to a Kosterlitz–Thouless transition where intersecting spin folds bind together in the low temperature phase. Even a weak anisotropy produces a rapid crossover from a low density to a high density of bound defects, and consequently a critical transition.

The kagome spin glass phase has several contrasts with conventional site-disordered spin glasses. Most obviously, the successive creation of the spin folds is non-Abelian, an algebra that creates a memory of all the ground states that were traversed [45, 47]. Also, the spin configurations retain the 120° ground state rule at all times. The energy landscape of the magnet is therefore translationally uniform, despite the disordered spin chirality—a remarkable symmetry that allows a hidden channel for the low energy Goldstone modes to occur in the kagome spin glass.

The model kagome antiferromagnet, hydronium jarosite $(H_3O)Fe_3(SO_4)_2(OH)_6$, has attracted considerable attention as it displays an unconventional spin glass-like phase [45, 48–50]. Two of its most remarkable properties are its magnetic specific heat that is quadratic with temperature, characteristic of Goldstone modes in a 2D antiferromagnet, rather than the linear response expected for a disordered spin glass [46], and the failure of temperature cycling phase to erase the memory of spin relaxations in the glassy phase [45, 50]. Both of these observations are elegantly explained by the kagome spin glass model and promote hydronium jarosite as an important model system with which to explore both the nature of spin glasses and the way in which macroscopic degeneracies can lead to complex out-of-equilibrium phases.

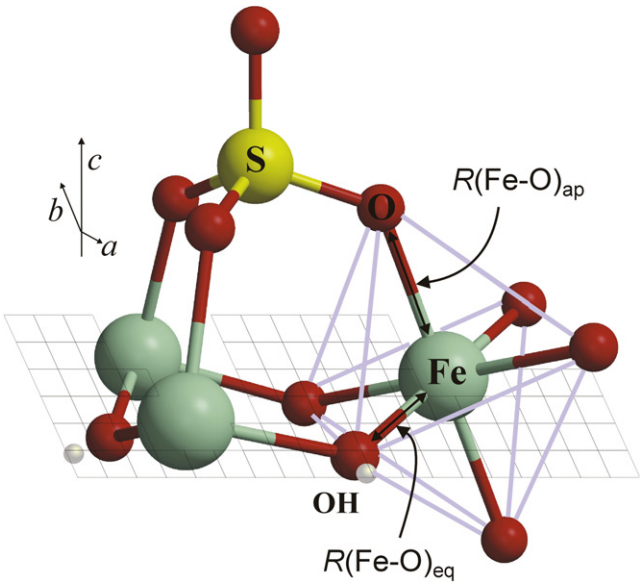

Figure 2. The local coordination of the magnetic Fe^{3+} ions. The apical Fe–O bond is slightly longer than the equatorial Fe–O bond. This distortion may be characterized by the ratio of bond lengths, $\Delta = 1 - R(\text{Fe–O})_{\text{eq}}/R(\text{Fe–O})_{\text{ap}}$.

The jarosite crystal structure is best described in the space group $R\bar{3}m$ and has the general formula $AFe_3(SO_4)_2(OH)_6$, ($A = H_3O^+$, NH_4^+, K^+, Na^+, Rb^+, Ag^+, $\frac{1}{2}Pb^{2+}$ or $\frac{1}{2}Tl^{2+}$) [51]. The Fe^{3+}, $S = \frac{5}{2}$, ions make up a series of translationally related kagome layers with an—ABC—stacking arrangement. These layers are sufficiently well separated, R(Fe–Fe)interlayer ~5.64 Å, that the magnetic Hamiltonian may be considered essentially 2D, which is confirmed by our following observations. The magnetic exchange between Fe ions is mediated through the bridging hydroxyl groups (figure 2) and the nearest neighbour distance is R(Fe–Fe)intralayer ~3.67 Å. There is a markedly different behaviour between the hydronium and non-hydronium jarosites with all of the non-hydronium jarosites ordering at low temperatures into a long-ranged Néel state with the propagation vector $\boldsymbol{k} = (0\ 0\ \frac{3}{2})$, with respect to the hexagonal setting of the space group [35]. Whether or not this ordering process is one or two staged appears sample dependent [52]. In all cases, however, the lower temperature transition occurs at $T_{N1} \sim 55$ K [35]. Hydronium

jarosite is quite different from the non-hydronium jarosites as it displays a critical spin glass transition at $T_g \sim 17$ K [45]. The short-ranged spin correlations increase only slowly upon cooling through this transition [53] and μ SR indicates that the maximum static moment at low temperature is 3.4 μ_B [54].

The hydronium jarosites were synthesized under standard hydrothermal synthesis conditions [51]. 2 g of $Fe_2(SO_4)_3$ were dissolved in 15 ml of water/methanol [55] solutions and heated at different temperatures between 120 and 150 °C for 21 h in Pyrex tubes with PTFE screw caps. The non-hydronium jarosites were synthesized using redox methods where iron wire is oxidized. [36, 56] The following $K_2(SO_4)_2$ (2.44 g, 0.28 mol), and $(NH_4)_2(SO_4)_2$ (1.85 g, 0.28 mol) were each dissolved and made up to 25 cm^3 with distilled water, to which 1.1 cm^3 of concentrated H_2SO_4 was added. For each reaction 0.336 g of iron wire, 2 mm diameter, 99.9% were put with the relevant A-site sulfate solution into a Pyrex tube (38 cm^3 total capacity). The reaction took place at 170 °C over 48 h. Magnetic susceptibility data were collected using a SQUID magnetometer in a field of 100 G. Single crystal x-ray diffraction data were taken at 80(2) K using an Oxford Cryostream and Mo $K\alpha_1$ radiation (0.710 73 Å). The data for the potassium jarosite was taken at the Daresbury SRS facility with x-rays of wavelength 0.6893 Å at 85(2) K. Position and peak intensities were extracted from the raw data using DENZO SMN and scaled using SCALEPACK; SADABS was used for adsorption correction. SHELX-97 [57] was used for structure solution and refinement. While the stoichiometry differences between these samples were too small to be resolved by chemical analysis or crystal structure refinement, the latter confirm that the Fe occupancy was >94% for all samples studied. This insensitivity of the magnetic properties to Fe occupancy [58] leads us to suggest that the following crystallographic changes are the result of a dependency of the A-site hydration number with synthesis conditions [56] that affects the distribution of protons between the A-site and the bridging hydroxide during jarosite formation. The connectivity of the lattice causes these changes at the A-site to compress or elongate the Fe-coordination octahedron.

Our studies of the single crystal diffraction data reveal small changes in the geometry of the Fe-coordination octahedra that correlate with the spin glass freezing temperature, T_g. The Fe^{3+} ions occupy the 9d positions of $R\bar{3}m$ and have point symmetry $2/m$. They are coordinated by 4 hydroxyl oxygen atoms in the equatorial (eq) plane and 2 apical (ap) oxygen atoms from the sulfate groups as shown in figure 2. The apical Fe–O bond is slightly longer than the equatorial bond and the distortion away from octahedral symmetry may be characterized by deviation of the ratio of bond lengths from unity: $\Delta = 1 - [R(\text{Fe–O})_{eq}/R(\text{Fe–O})_{ap}]$. Figure 3 shows an apparent linear dependence of T_g with the ratio Δ: the samples that have more distorted Fe-octahedra display larger values of T_g. As Δ is derived from Bragg diffraction, it represents an ordered crystallographic distortion. The spin glass transition in hydronium jarosite is therefore the result of an ordered energy scale associated with Δ and it is not the simple result of random disorder, as has been suggested [59, 60].

It should be noted that concomitant with an increase in the crystallographic c-axis as the kagome layers are pushed apart

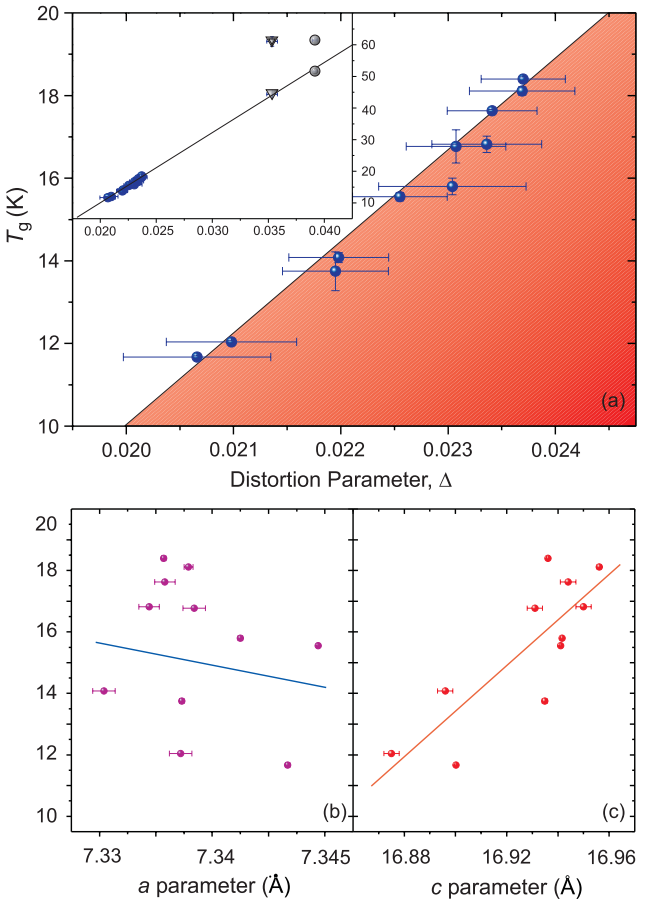

Figure 3. (a) The relation between the critical spin glass freezing transition in hydronium jarosite, T_g, and the distortion parameter, $\Delta = 1 - R(\text{Fe–O})_{eq}/R(\text{Fe–O})_{ap}$. The more distorted the Fe-octahedra, the higher the transition temperature. The approximately linear correlation suggests that the anisotropy responsible for the spin glass transition is proportional to the extent of the distortion. The inset shows that the same linear function fitted for hydronium jarosite can be extended to the antiferromagnetic Néel ordering temperatures of $(NH_4)Fe_3(SO_4)_2(OH)_6$ (grey triangles) and $KFe_3(SO_4)_2(OH)_6$ (grey circles). (b) and (c) show that the distortion largely relates to changes in the c-lattice parameter. The expansion along c caused by increasing distortion corresponds to a pushing apart of the kagome layers. The concomitant increase in T_g indicates that the interlayer exchange is not responsible for the spin glass transition.

(figure 3(c)), reducing interlayer coupling. The related increase in T_g proves that the interlayer interactions are not responsible for the spin glass phase, stressing the quasi-2D nature of this KAFM.

This relationship between the local distortion of the Fe^{3+} and the magnetic ordering is reinforced by studies of the non-hydronium jarosites which show Néel order. All these jarosites possess far greater distortions away from octahedral symmetry than the hydronium member, and correspondingly higher antiferromagnetic transition temperatures. The inset of figure 3(a) shows an extrapolation of the linear dependence of T_g with $R(\text{Fe–O})_{eq/ap}$ observed in hydronium jarosite. Excellent agreement between this trend and the lower temperature transitions of $(NH_4)Fe_3(SO_4)_2(OH)_6$ (T_{N2} =

43.0 (5) K, $T_{N1} = 61.0$ (5) K, $\Delta = 0.03534$ (48)) and $KFe_3(SO_4)_2(OH)_6$ ($T_{N2} = 51.7$ (5) K, $T_{N1} = 61.5$ (5) K, $\Delta = 0.03916$ (20)) evidences a common energy scale between the ordering transitions in the hydronium and the non-hydronium iron jarosites, which is all the more remarkable given the different natures of the orderings. The underlying similarities of the energy scales responsible for the kagome spin glass and the ordered Néel states of the jarosites then indicates that hydronium jarosite is on the verge of Néel order and that the nature of the low temperature phase is controlled by Δ. This mechanism also provides an explanation for the remarkable 'order-by-disorder' effect observed following substitution of Al^{3+} for Fe^{3+} in hydronium jarosite [61].

Recent Mössbauer spectroscopy measurements have shown the Fe^{3+} spins in the spin glass phase of hydronium jarosite lie in the kagome plane [62], confirming the presence of an effective planar anisotropy. The data shown in figure 3 indicate that in the jarosites, the anisotropy is enhanced by increasing large distortion, Δ, away from octahedral symmetry. As Fe^{3+} would naïvely expected to be $S = \frac{5}{2}$ and $L = 0$, the origin of this magnetocrystalline anisotropy is unclear. Several energy terms could be involved, e.g. anisotropic exchange, dipolar energy, the Dzyaloshinsky–Moriya (DM) interaction [63, 64], or mixing-in of excited contributions within the $3d^5$ electronic states [65, 66]. Unfortunately, the nature of a spin glass and the strong microwave absorption by H_3O^+ makes difficult the determination of which is implicated.

Spin wave analysis of potassium jarosite, which shows Néel order below successive transitions at $T \sim 60$ K, indicates that a significant DM component, is present at low temperatures [67]. It is reasonable to conclude that the presence of a similar component in hydronium jarosite would also lead to Néel order, crystallizing the lowest energy chiral state from the degenerate manifold. It therefore appears that another anisotropy term is present which leads to transition to the spin glass-like state in this material. Further, the relationship between transition temperature and the distortion, Δ, implicates this anisotropy term in the Néel ordering of the other jarosites.

In conclusion, we show that the KAFM hydronium jarosite displays a remarkable glass-like magnetic state. The underlying basis for this phase is unlike that of conventional spin glasses as it appears not from random disorder, but from a regular planar anisotropy which retards the evolution through the highly degenerate ground state. The stark simplicity of this model KAFM may therefore provide important insights into one of the long-standing questions in condensed matter physics—the nature of the spin glass transition—and more generally help our understanding of the analogous out-of-equilibrium dynamics found in diverse systems such as spin glasses, high T_C superconductors, neural networks and protein folding.

This work has been funded by the Royal Society and EPSRC grant number EP/C534654/1. We would like to thank PCW Holdsworth and ST Bramwell for discussions; the ENS Lyon for provision of travel funds; and the UK National Crystallography Service (NCS), along with the assistance of S Coles and W Clegg.

References

[1] Anderson P W 1983 *Proc. Natl Acad. Sci. USA* **80** 3386
[2] Anderson P W and Abrahams E 1987 *Nature* **327** 363
[3] Ramirez A P 2003 *Nature* **421** 483
[4] Schiffer P, Ramirez A P, Huse D A, Gammel P L, Yaron U, Bishop D J and Valentino A J 1995 *Phys. Rev. Lett.* **74** 2379
[5] Dunsiger S R, Gardner J S, Chakhalian J, Cornelius A L, Jaime M, Kiefl R F, Movshovich R, MacFarlane W A, Miller R I, Sonier J E and Gaulin B D *Phys. Rev. Lett.* **85** 3504
[6] Petrenko O A, Balakrishnan G, Paul D McK, Yethiraj M and Klenke J 2002 *Appl. Phys.* A **74** S760
[7] Raju N P, Dion M, Gingras M J P, Mason T E and Greedan J E 1999 *Phys. Rev.* B **59** 14489
[8] Bonville P, Hodges J A, Ocio M, Sanchez J P, Vulliet P, Sosin S and Braithwaite D 2003 *J. Phys.: Condens. Matter* **15** 7777
[9] Champion J D M, Wills A S, Fennell T, Bramwell S T, Gardner J S and Green M A 2001 *Phys. Rev.* B **64** 140407
[10] Stewart J R, Ehlers G, Wills A S, Bramwell S T and Gardner J S 2004 *J. Phys.: Condens. Matter* **16** L321
[11] Wills A S, Zhitomirsky M E, Canals B, Sanchez J P, Bonville P, Dalmas de Réotier P and Yaouanc A 2006 *J. Phys.: Condens. Matter* **18** L37
[12] Champion J D M, Harris M J, Holdsworth P C W, Wills A S, Balakrishnan G, Bramwell S T, Čižmár E, Fennell T, Gardner J S, Lago J, Mcmorrow D F, Orendáč M, Orendáčová A, Paul D McK, Smith R I, Telling M T F and Wildes A 2003 *Phys. Rev.* B **68** 4
[13] Poole A, Wills A S and Lelièvre-Berna E 2007 *J. Phys.: Condens. Matter* **19** 452201
[14] Raju N P, Gmelin E and Kremer R K 1992 *Phys. Rev.* B **46** 5405
[15] Gingras M J P, Stager C V, Gaulin B D, Raju N P and Greedan J E 1996 *J. Appl. Phys.* **79** 6170
[16] Lee J S, Noh T W, Bae J S, Yang I S, Takeda T and Kanno R 2004 *Phys. Rev.* B **69** 214428
[17] Greedan J E, Raju N P, Wills A S, Morin C, Shaw S M and Reimers J N 1998 *Chem. Mater.* **10** 3058
[18] Wills A S, Raju N P and Greedan J E 1999 *Chem. Mater.* **11** 1510
[19] Greedan J E, Wiebe C R, Wills A S and Stewart J R 2002 *Phys. Rev.* B **65** 184424
[20] Wiebe C R, Russo P L, Savici A T, Uemura Y J, Macdougall G J, Luke G M, Kuchta S and Greedan J E 2005 *J. Phys.: Condens. Matter* **17** 6469
[21] Wills A S, Raju N P, Morin C and Greedan J E 1999 *Chem. Mater.* **11** 1936
[22] Klemme S and Miltenburg J C V 2004 *Mineral. Mag.* **68** 515
[23] Lee S H, Broholm C, Ratcliff W, Gasparovic G, Huang Q, Kim T H and Cheong S W 2002 *Nature* **418** 856
[24] Parker D R, Green M A, Bramwell S T, Wills A S, Gardner J S and Neumann D A 2004 *J. Am. Chem. Soc.* **126** 2710
[25] Pinsard-Gaudart L, Dragoe N, Lagarde P, Flank A M, Itie J P, Congeduti A, Roy P, Niitaka S and Takagi H 2007 *Phys. Rev.* B **76** 045119
[26] Hemberger J, Krug von Nidda H-A, Tsurkan V and Loidl A 2007 *Phys. Rev. Lett.* **98** 147203
[27] Limot L, Mendels P, Collin G, Mondelli C, Ouladdiaf B, Mutka H, Blanchard N and Mekata M 2002 *Phys. Rev.* B **65** 144447
[28] Mutka H, Ehlers G, Payen C, Bono D, Stewart J R, Fouquet P, Mendels P, Mevellec J Y, Blanchard N and Collin G 2006 *Phys. Rev. Lett.* **97** 047203
[29] Hagemann I S, Huang Q, Gao X P A, Ramirez A P and Cava R J 2001 *Phys. Rev. Lett.* **86** 894
[30] Lawes G, Kenzelmann M, Rogado N, Kim K H, Jorge G A, Cava R J, Aharony A, Entin-Wohlman O, Harris A B, Yildrim T, Huang Q, Park S, Broholm C and Ramirez A P 2004 *Phys. Rev. Lett.* **93** 247201

[31] Lancaster T, Blundell S J, Baker P J, Prabhakaran D, Hayes W and Pratt F 2007 *Phys. Rev.* B **75** 064427
[32] Wilson N R, Petrenko O A and Balakrishnan G 2007 *J. Phys.: Condens. Matter* **19** 145257
[33] Lee S H, Broholm C, Collins M F, Heller L, Ramirez A P, Kloc C, Bucher E, Erwin R W and Lacevic N 1997 *Phys. Rev.* B **56** 8091
[34] Inami T, Nishiyama M, Maegawa S and Oka Y 2000 *Phys. Rev.* B **61** 12181
[35] Wills A S 2001 *Can. J. Phys.* **79** 1501
[36] Grohol D, Nocera D and Papoutsakis D 2003 *Phys. Rev.* B **67** 064401
[37] Wills A S, Raymond S and Henry J Y 2004 *J. Magn. Magn. Mater.* **272–276** 850
[38] Zheng X G, Kubozono H, Nishiyama K, Higemoto W, Kawae T, Koda A and Xu C N 2005 *Phys. Rev. Lett.* **95** 057201
[39] Zheng X G, Kawae T, Kashitani Y, Li C S, Tateiwa N, Takeda K, Yamada H, Xu C N and Ren Y 2005 *Phys. Rev.* B **71** 052409
[40] Shores M P, Nytko E A, Bartlett B M and Nocera D G 2005 *J. Am. Chem. Soc.* **127** 13462
[41] Harris M J, Bramwell S T, Holdsworth P C W and Champion J D M 1998 *Phys. Rev. Lett.* **81** 4496
[42] Wang R F, Nisoli C, Freitas R S, Li J, McConville W, Cooley B J, Lund M S, Samarth N, Leighton C, Crespi V H and Schiffer P 2006 *Nature* **439** 303
[43] Qi Y, Brintlinger T and Cumings J 2008 *Phys. Rev.* B **77** 094418
[44] Wills A S, Ballou R and Lacroix C 2002 *Phys. Rev.* B **66** 144407
[45] Wills A S, Dupuis V, Vincent E, Hammann J and Calemczuk R 2000 *Phys. Rev.* B **62** R9264
[46] Mydosh J A 1995 *Spin Glasses: An Experimental Introduction* (London: Taylor and Francis)
[47] Ritchey I, Chandra P and Coleman P 1993 *Phys. Rev.* B **47** 15342
[48] Wills A S and Harrison A 1996 *J. Chem. Soc. Faraday* T **92** 2161
[49] Wills A S, Harrison A, Mentink S A M, Mason T E and Tun Z 1998 *Europhys. Lett.* **42** 325
[50] Dupuis V, Vincent E, Hammann J, Greedan J E and Wills A S 2002 *J. Appl. Phys.* **91** 8384
[51] Dutrizac J and Kaiman S 1976 *Can. Miner.* **14** 151
[52] Frunzke J, Hansen T, Harrison A, Lord J S, Oakley G S, Visser D and Wills A S 2001 *J. Mater. Chem.* **11** 179
[53] Wills A S, Oakley G S, Visser D, Frunzke J, Harrison A and Andersen K H 2001 *Phys. Rev.* B **64** 094436
[54] Harrison A, Kojima K M, Wills A S, Fudamato Y, Larkin M I, Luke G M, Nachumi B, Uemura Y J, Visser D and Lord J S 2000 *Physica* B **289–290** 217
[55] Earle S A, Ramirez A P and Cava R J 1999 *Physica* B **262** 199
[56] Bisson W and Wills A S 2007 *Z. Kristallogr. Suppl.* **26** 511
[57] Sheldrick G M 1997 *Shelx97, Programs for Crystal Structure Analysis* (release 97-2)
[58] Bisson W G and Wills A S, unpublished work
[59] Grohol D and Nocera D G 2007 *Chem. Mater.* **19** 3061
[60] Fåk B, Coomer F C, Harrison A, Visser D and Zhitomirsky M E 2007 *Europhys. Lett.* **81** 17006
[61] Wills A S, Harrison A, Ritter C and Smith R I 2000 *Phys. Rev.* B **61** 6156
[62] Bonville P, Dupuis V, Vincent E, Lippens P E and Wills A S 2006 *Hyperfine Interact.* **168** 1085
[63] Dzyaloshinski I E 1958 *J. Phys. Chem. Solids* **4** 241
[64] Moriya T 1960 *Phys. Rev. Lett.* **4** 228
[65] Abragam A and Bleaney B 1970 *Electron Paramagnetic Resonance of Transition Ions* (Oxford: Clarendon)
[66] Geschwind S 1961 *Phys. Rev.* **121** 363
[67] Yildirim T and Harris A B 2006 *Phys. Rev.* B **73** 214446